

# Electron Transport Chain-dependent and -independent Mechanisms of Mitochondrial H<sub>2</sub>O<sub>2</sub> Emission during Long-chain Fatty Acid Oxidation<sup>\*[5]</sup>

Received for publication, May 27, 2009, and in revised form, December 18, 2009. Published, JBC Papers in Press, December 23, 2009, DOI 10.1074/jbc.M109.026203

Erin L. Seifert, Carmen Estey, Jian Y. Xuan, and Mary-ellen Harper<sup>1</sup>

From the Department of Biochemistry, Microbiology, and Immunology, Faculty of Medicine, University of Ottawa, Ottawa, Ontario K1H 8M5, Canada

Oxidative stress in skeletal muscle is a hallmark of various pathophysiological states that also feature increased reliance on long-chain fatty acid (LCFA) substrate, such as insulin resistance and exercise. However, little is known about the mechanistic basis of the LCFA-induced reactive oxygen species (ROS) burden in intact mitochondria, and elucidation of this mechanistic basis was the goal of this study. Specific aims were to determine the extent to which LCFA catabolism is associated with ROS production and to gain mechanistic insights into the associated ROS production. Because intermediates and by-products of LCFA catabolism may interfere with antioxidant mechanisms, we predicted that ROS formation during LCFA catabolism reflects a complex process involving multiple sites of ROS production as well as modified mitochondrial function. Thus, we utilized several complementary approaches to probe the underlying mechanism(s). Using skeletal muscle mitochondria, our findings indicate that even a low supply of LCFA is associated with ROS formation in excess of that generated by NADH-linked substrates. Moreover, ROS production was evident across the physiologic range of membrane potential and was relatively insensitive to membrane potential changes. Determinations of topology and membrane potential as well as use of inhibitors revealed complex III and the electron transfer flavoprotein (ETF) and ETF-oxidoreductase, as likely sites of ROS production. Finally, ROS production was sensitive to matrix levels of LCFA catabolic intermediates, indicating that mitochondrial export of LCFA catabolic intermediates can play a role in determining ROS levels.

Reactive oxygen species (ROS)<sup>2</sup> are generated in mitochondria as a normal byproduct of aerobic metabolism; 0.2–2% of O<sub>2</sub>

consumption is estimated to be lost as superoxide under normal conditions (1, 2). Within the mitochondrial matrix, a suite of enzymes manages the ROS load by converting ROS to less toxic species or by mitigating their formation. Nevertheless, mitochondria are significant sources of cellular ROS, and oxidative stress is a hallmark of various physiological and pathological states, including exercise, insulin resistance, and atherosclerosis (3–10).

Inhibitor studies in mitochondria utilizing NADH- or FADH<sub>2</sub>-linked substrates suggest that complexes I and III of the electron transport chain (ETC) are predominant sites of superoxide production (11–13). Whether this is the case under physiologic conditions is not well appreciated. ROS generation by the ETC is critically dependent upon ETC redox state, such that ROS production is low until the inner membrane is significantly polarized and then rises steeply with small increments in membrane potential (14). However, a membrane potential-independent component of ROS production has been observed in brain mitochondria (15–17). Indeed, electrons may escape from sites other than the respiratory complexes, such as from the electron transfer flavoprotein (ETF) and ETF-ubiquinone oxidoreductase (ETF-QO) (18) or the  $\alpha$ -ketoglutarate dehydrogenase complex (19–21). Finally, the mitochondrial ROS load also depends upon the activity of antioxidant processes. Thus, net mitochondrial ROS load is a complex function of several factors.

ROS production during catabolism of long-chain fatty acids (LCFA; refer to the [supplementary material](#) for a list of non-standard abbreviations) may reflect a particularly complex process (Fig. 1). Compared with non-FA substrates, the generation of reducing equivalents is high during LCFA catabolism: fatty acid oxidation (FAO) and yields both NADH and FADH<sub>2</sub>. In addition, the dehydrogenases of  $\beta$ -oxidation can transfer electrons to the ETF, which then reduces ETF-QO with the possibility of electron leakage from both sites. Finally, LCFA breakdown can generate intermediates and by-products that can inhibit matrix enzymes that mitigate or detoxify ROS (22–25). Intermediates can also inhibit the ETC to potentially augment ROS production (26–28). It is unknown which factor(s) have the greatest influence on ROS formation during FAO. This question is of interest because some pathophysiological conditions that feature oxidative stress, such as insulin resistance and type 2 diabetes, are also associated with altered FAO

\* This work was supported by the Canadian Institutes of Health Research (Institute of Nutrition, Metabolism, and Diabetes) (to M.-E.H.) and by a fellowship from the Canadian Diabetes Association (to E. L. S.). Part of this work was presented at the Obesity Society Meeting, 2007.

[5] The on-line version of this article (available at <http://www.jbc.org>) contains [supplemental Table 1](#) and [Figs. 1–5](#).

<sup>1</sup> To whom correspondence should be addressed: Dept. of Biochemistry, Microbiology, and Immunology, Faculty of Medicine, University of Ottawa, 451 Smyth Rd., Ottawa, Ontario K1H 8M5, Canada. Tel.: 613-562-5800 (ext. 8235); Fax: 613-562-5452; E-mail: Maryellen.Harper@uottawa.ca.

<sup>2</sup> The abbreviations used are: ROS, reactive oxygen species; ETC, electron transport chain; ETF, electron transfer flavoprotein; ETF-QO, ETF-ubiquinone oxidoreductase; LCFA, long-chain fatty acid(s); CDNB, 1-chloro-2,4-dinitrobenzene; PCarn, palmitoylcarnitine; PHPA, *p*-hydroxyphenylacetate; P/M, pyruvate/malate; G/M, glutamate/malate; TPMP<sup>+</sup>, methyl-triphenyl-phosphonium; FCCP, *p*-trifluoromethoxy carbonyl cyanide phenyl

hydrazine; ASP, acid-soluble product; SOD, superoxide dismutase; RET, reverse electron transport; FAO, fatty acid oxidation.

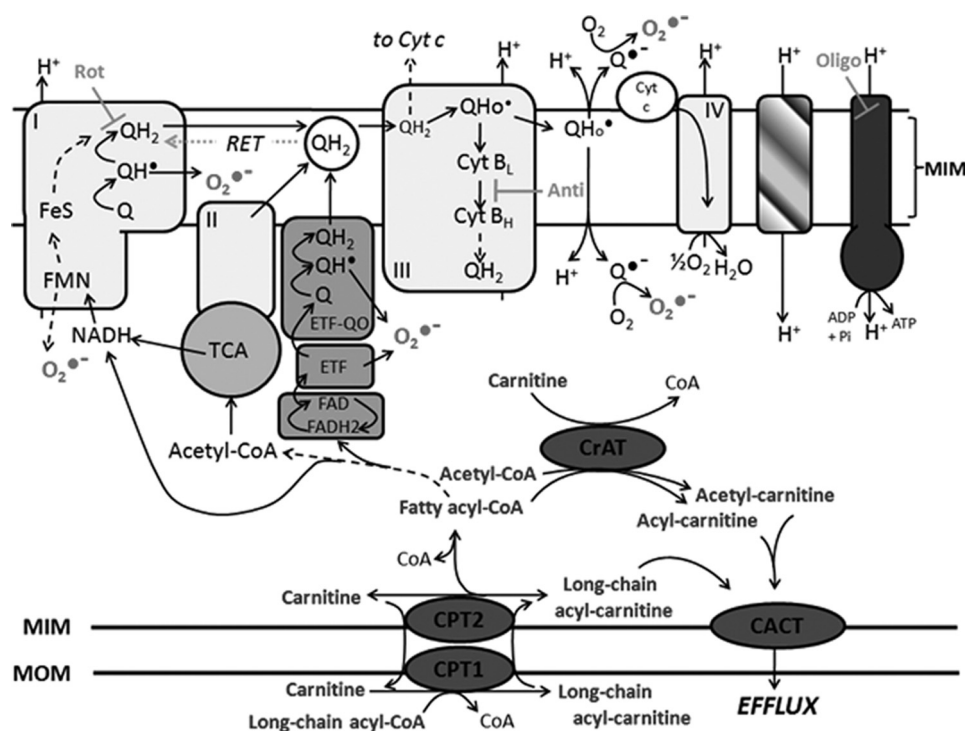


**FIGURE 1. Mitochondrial fatty acid handling and possible mechanisms of ROS generation during fatty acid oxidation.** LCFA are activated on the mitochondrial outer membrane (MOM) to acyl-CoA and then taken up into mitochondria by the carnitine palmitoyltransferase (CPT) system, with conversion to acylcarnitine and then back to acyl-CoA. Electrons enter the ETC via  $\beta$ -oxidation and the tricarboxylic acid cycle (TCA) or via the ETF and ETF-QO. Possible sites of electron leakage and ROS formation are at complex I (at the flavin site or at the quinone binding site via RET) (13, 44, 54), at complex III (13, 51, 53), and from the ETF and ETF-QO (18). ROS generated at complex III can diffuse into the matrix and the intermembrane space (13, 51). If acyl-CoA supply exceeds the downstream catabolic capacity, acyl-CoA esters can be converted to acylcarnitines via carnitine acyltransferase (CrAT; with specificity for acetyl-CoA and short-chain acyl-CoA) and then exported from mitochondria via carnitine acylcarnitine transferase (CACT) (62). L-Carnitine supplementation increases acylcarnitine export (55–57). Because acyl-CoA esters can inhibit matrix ROS mitigating or detoxifying enzymes (22–25), acylcarnitine export may lower ROS during FAO. Rotenone (Rot) inhibits complex I. Antimycin A (Anti) binds cytochrome *b* to prevent electron flow to the ubiquinone binding site of complex III. Oligomycin (Oligo) inhibits the ATP synthase. MIM, mitochondrial inner membrane.

capacity, increased reliance on LCFA substrate, or increased incomplete FAO (29–33), yet there has been little investigation into the mechanistic basis of the LCFA-induced ROS. A major limitation of studies that have attempted to address the mechanistic basis of ROS production during FAO is that they have utilized high concentrations of FA substrate and relied exclusively upon complex I and III inhibitors as tools (13, 34).

Thus, the aims of the present study were 1) to determine the extent to which low, more physiologic [LCFA] can generate ROS and 2) to characterize the associated mechanisms using several complementary approaches (membrane potential determinations, ETC inhibition, L-carnitine supplementation to lower matrix acyl-CoA levels (see Fig. 1), and glutathione depletion). Due to the association between ROS and insulin resistance in skeletal muscle (4, 5), we focused on mitochondria from this tissue. For comparative purposes, some experiments were also performed in liver mitochondria. Our findings indicate that even a low [LCFA] is associated with ROS formation in excess of that generated by oxidation of NADH-linked substrates. Observations support complex III, not complex I, as an important site of ROS formation during FAO. Moreover, we identify a membrane potential-independent component, which may be partially due to ROS generated at the ETF/ETF-QO.

Finally, we demonstrate that ROS production is sensitive to levels of matrix LCFA catabolic intermediates, indicating a role for the latter in determining the LCFA-induced ROS burden.

## EXPERIMENTAL PROCEDURES

**Reagents**—[1-<sup>14</sup>C]Palmitoylcarnitine was purchased from Perkin-Elmer Life Sciences. All other reagents were obtained from Sigma. Reagents were dissolved in incubation medium (see below for composition) or distilled H<sub>2</sub>O, except for oligomycin, rotenone, antimycin, 1-chloro-2,4-dinitrobenzene (CDNB), and *p*-trifluoromethoxy carbonyl cyanide phenyl hydrazone (FCCP), which were dissolved in EtOH. Stocks of palmitoylcarnitine (PCarn), glutamate, and malate were stored for up to 1 month at –20 or –80 °C (PCarn). Pyruvate was prepared immediately prior to use.

**Animals**—Male C57Bl/6J mice, 4–6 months of age, were obtained from our colony and housed in our facility at 23 °C (12 h/12 h light cycle, lights on at 0700 h), with free access to water and chow (6% fat/weight; Harlan-Teklad-2018). Additional age-matched male C57Bl/6 mice were obtained from Charles River and acclimated to our facility

for  $\geq 3$  weeks prior to experimentation. Animals were cared for in accordance with the principles and guidelines of the Canadian Council on Animal Care and the Institute of Laboratory Animal Resources (National Research Council). This study was approved by the Animal Care Committee of the University of Ottawa.

**Isolation of Mitochondria from Skeletal Muscle and Liver**—Muscle mitochondria were isolated essentially according to Chappell and Perry (35), as described (36) (supplemental material). Liver mitochondria were isolated using a standard protocol (37) (supplemental material). Protein concentration was determined by a modified Lowry method using bovine serum albumin as the standard.

All experiments were conducted in incubation medium containing 120 mM KCl, 1 mM EGTA, 5 mM KH<sub>2</sub>PO<sub>4</sub>, 5 mM MgCl<sub>2</sub>, and 5 mM HEPES, pH 7.4, supplemented with 0.3% defatted bovine serum albumin. Unless otherwise stated, determinations were made in the presence of oligomycin (3  $\mu$ g/ml) to inhibit ATP synthesis, a condition used in previous studies of the mechanisms of ROS formation in isolated mitochondria and permeabilized muscle fibers (e.g. see Refs. 4, 13, 34, and 38). Measurements in muscle and liver mitochondria were made in parallel from mitochondria isolated from the same mouse.

## Mechanisms of ROS Generation during LCFA Catabolism

**Hydrogen Peroxide Emission Rate**—The  $\text{H}_2\text{O}_2$  emission rate was measured fluorimetrically using *p*-hydroxyphenylacetate (PHPA; 167  $\mu\text{g}/\text{ml}$ ) and horseradish peroxidase (9 units/ml) (37, 39) in mitochondria (0.2 mg/ml) suspended in incubation medium.  $\text{H}_2\text{O}_2$  emission was monitored for up to 30 min at 37 °C using a temperature-controlled fluorimeter (excitation at 320 nm, emission at 400 nm) (FLx800, BioTek).  $\text{H}_2\text{O}_2$  rates were calculated using a calibration curve constructed in the presence of mitochondria (which quench the fluorescence). Note that  $\text{O}_2$  consumption for each substrate used was measurable under state 4 conditions for  $\geq 30$  min. In the presence of complex I or III inhibitors or with succinate alone, the  $\text{H}_2\text{O}_2$  emission rate was biphasic, with an initial linear phase lasting  $\sim 10$  min, followed by a slower prolonged phase; only the initial phase was analyzed. Although Amplex Red conversion to fluorescent resorufin may be a more sensitive detector of  $\text{H}_2\text{O}_2$  than PHPA, we have detected artifactual rates with Amplex Red, possibly due to the generation of a resorufin signal by reaction of Amplex Red with FA hydroperoxides (40). We thus opted to use the PHPA method. Apparent reagent-only rates of  $\text{H}_2\text{O}_2$  have been reported with a similar assay utilizing homovanillic acid (13). We monitored fluorescence for all combinations of reagents and substrates; no systematic changes were detected. Catalase (100 units/ml) was used to confirm that changes in fluorescence were due to  $\text{H}_2\text{O}_2$ .

**Oxygen Consumption**—Oxygen consumption was measured in mitochondria (0.2 mg/ml) at 37 °C using a Clark-type  $\text{O}_2$  electrode (Hansatech, Norfolk, UK) and incubated in incubation medium assumed to contain 406 nmol of oxygen/ml at 37 °C (41). Details of the different incubation conditions are provided under “Results.” Respiratory control ratios for muscle and liver mitochondria are provided in [supplemental Table 1](#). Respiratory control ratios of  $\sim 10$  and  $\sim 12$  for muscle mitochondria oxidizing pyruvate/malate (P/M; 10/5 mM) and glutamate/malate (G/M; 10/5 mM), respectively, and  $\sim 12$  for liver mitochondria oxidizing G/M (10/5 mM) indicate that mitochondria from both tissues were well coupled. Predictably, respiratory control ratios were lower with PCarn oxidation ( $\sim 5$ ), as was the respiratory control ratio of liver mitochondria oxidizing P/M ( $\sim 5$ ).

**Membrane Potential**—Membrane potential (measured as  $\Delta\psi$ ,  $\Psi\text{m}$ ) was determined in mitochondria (0.2 mg/ml), incubated in incubation medium at 37 °C, using a methyl-triphenyl-phosphonium (TPMP<sup>+</sup>)-selective electrode (37, 42) or fluorimetrically using safranin O dye (5  $\mu\text{M}$ ; excitation at 485 nm and emission at 580 nm) (43). The fluorimetric approach enabled simultaneous measurement of replicates under several conditions.

**NAD(P)H/NAD(P)<sup>+</sup> Redox State**—NAD(P)H autofluorescence (excitation at 365 nm, emission at 450 nm) was used to determine mitochondrial NAD(P)H/NAD(P)<sup>+</sup> (44) under incubation conditions identical to those used for  $\text{H}_2\text{O}_2$  and bioenergetic determinations. Maximal oxidation and reduction were defined, respectively, as the fluorescence obtained in the presence of FCCP (0.6  $\mu\text{M}$ ) and rotenone (5  $\mu\text{M}$ ).

**Metabolites of FAO**—Rates of  $^{14}\text{C}$ -labeled acid-soluble product (ASP) formation and  $^{14}\text{CO}_2$  production were measured in muscle and liver mitochondria oxidizing [1- $^{14}\text{C}$ ]palmitoylcar-

nitine as described (36) ([supplemental material](#)). The reaction was initiated by adding mitochondria (0.2 mg/ml), and terminated by adding 70% perchloric acid. Half of the reaction volume was used to determine  $^{14}\text{CO}_2$  production. The other half was removed by syringe from the sealed vessel into a 1.5-ml tube, and mitochondria were pelleted at  $12,000 \times g$  for 5 min. The buffer and mitochondrial fractions were analyzed for [ $^{14}\text{C}$ ]ASP.

**Data Analysis**—All measurements were performed in duplicate, and replicates were averaged. Data are presented as the mean  $\pm$  S.E. A paired or unpaired *t* test or one-way or two-way analysis of variance was performed as appropriate using GraphPad Prism version 4 software (GraphPad Software, Inc., La Jolla, CA).

## RESULTS

**Low Concentrations of LCFA Substrate Generate ROS**—Skeletal muscle and cardiac mitochondria supplied with high [PCarn] (60  $\mu\text{M}$ ) were found to emit  $\text{H}_2\text{O}_2$  at a greater rate than when oxidizing P/M (13). However, greater  $\text{H}_2\text{O}_2$  emission during oxidation of high [PCarn] in muscle mitochondria is not a consistent finding (34). We wondered whether these discrepant results reflect the use of high [LCFA]. Indeed, [PCarn] as low as 5  $\mu\text{M}$  can inhibit ETC flux in skeletal muscle mitochondria (26). In addition, high [LCFA] can stimulate permeability transition (45, 46). Our first aim was to determine whether oxidation of lower, more physiologic [LCFA] could generate ROS at significant rates in skeletal muscle mitochondria.

$\text{H}_2\text{O}_2$  emission was clearly detectable with [PCarn] as low as 4.5  $\mu\text{M}$  and rose steadily for [PCarn] up to 18  $\mu\text{M}$  (Fig. 2A). Similar rates were obtained with 36  $\mu\text{M}$  as with 18  $\mu\text{M}$  PCarn. Interestingly, rates of  $\text{H}_2\text{O}_2$  emission were lower with 72  $\mu\text{M}$  PCarn as compared with rates measured with 18  $\mu\text{M}$ . The lower  $\text{H}_2\text{O}_2$  emission rate at high [PCarn] was not related to stimulation of permeability transition because mitochondrial swelling was not detectable with [PCarn] of  $< 100$   $\mu\text{M}$ , as determined spectrophotometrically at 540 nm (47) (not shown). It is well known that FA can directly uncouple respiration. To determine whether PCarn was uncoupling mitochondria, we preincubated (5 min) mitochondria with 18 or 72  $\mu\text{M}$  PCarn and then measured  $\text{H}_2\text{O}_2$  emission generated during reverse electron transport (RET), which is steeply dependent upon  $\Psi\text{m}$  (12, 48) ([supplemental Fig. 1](#)); if PCarn uncouples mitochondria, then PCarn would lower  $\text{H}_2\text{O}_2$  emission during RET.  $\text{H}_2\text{O}_2$  emission was found to be similar in the presence and absence of 18  $\mu\text{M}$  PCarn but was slightly decreased by 72  $\mu\text{M}$  PCarn ([supplemental Fig. 1C](#)). Thus, 18  $\mu\text{M}$  PCarn does not have an uncoupling effect, whereas 72  $\mu\text{M}$  PCarn may induce slight uncoupling. Thus, it is possible that the lower  $\text{H}_2\text{O}_2$  emission with 72  $\mu\text{M}$  PCarn (Fig. 2A) is due to a slight degree of uncoupling.

In contrast to PCarn,  $\text{H}_2\text{O}_2$  emission was undetectable with a supply of saturating P/M or G/M (Fig. 2B).  $\text{H}_2\text{O}_2$  emission was, however, apparent with these substrates upon the addition of the complex I inhibitor rotenone (see Fig. 4C), indicating the capacity for oxidation of these substrates to yield ROS.

**$\Psi\text{m}$ -Independent Component of  $\text{H}_2\text{O}_2$  Emission during PCarn Oxidation**—The mechanistic basis of ROS formation during LCFA catabolism is poorly understood. Because ROS

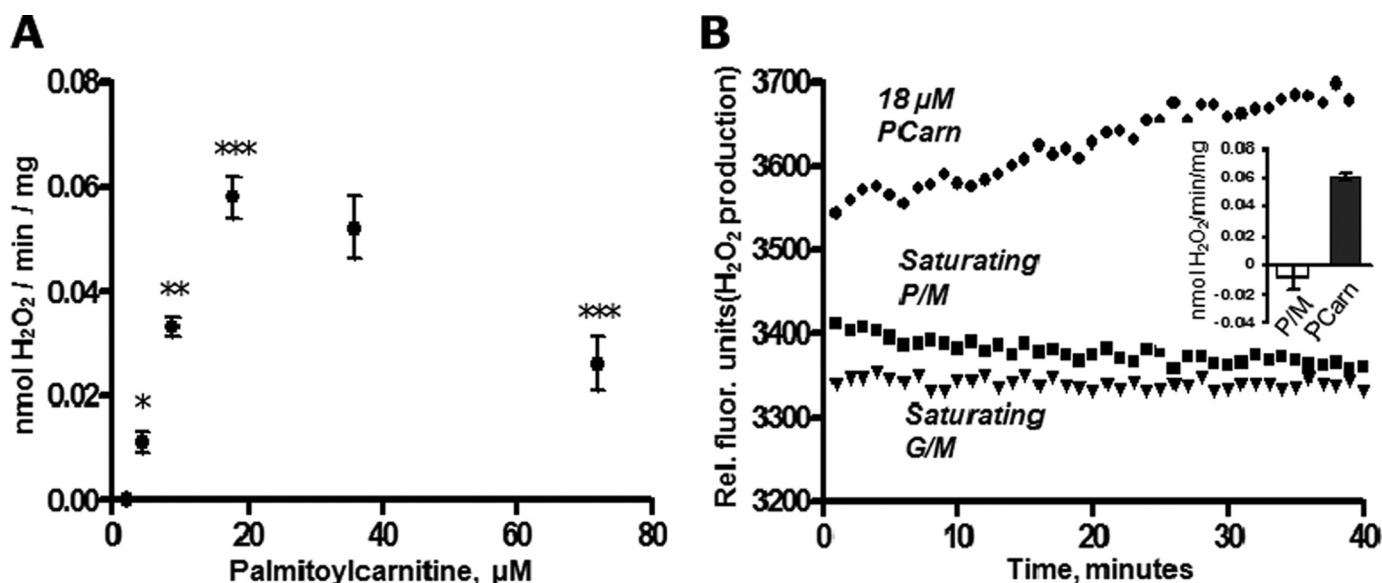


FIGURE 2.  $\text{H}_2\text{O}_2$  emission rate as a function of substrate concentration and type in skeletal muscle mitochondria. *A*,  $\text{H}_2\text{O}_2$  emission rate with increasing supply of PCarn. Values are means  $\pm$  S.E.,  $n = 5$  ( $n = 2$  for  $36 \mu\text{M}$  PCarn). \*, \*\*, and \*\*\*,  $p < 0.05$ ,  $p < 0.01$ , and  $p < 0.001$ , respectively, significantly different from adjacent lower concentration; one-way analysis of variance (repeated measures), Bonferroni post-tests; analysis excludes  $36 \mu\text{M}$  palmitoylcarnitine. *B*, raw fluorescence signals showing  $\text{H}_2\text{O}_2$  emission with  $18 \mu\text{M}$  palmitoylcarnitine but not with a saturating concentration of NADH-linked substrate (pyruvate/malate, 10/5 mM; glutamate/malate, 10/5 mM).  $\text{H}_2\text{O}_2$  emission is indicated by an increase in the fluorescence signal. *Inset*, quantification (nmol  $\text{H}_2\text{O}_2$ /min/mg). Open bar, pyruvate/malate; closed bar, PCarn. Values are means  $\pm$  S.E. ( $n = 5$ ).

formation by the ETC is favored when the ETC complexes are highly reduced (12, 14), we determined whether this might explain the elevated ROS production with PCarn. We assessed ETC redox status by monitoring  $\Psi\text{m}$  using a TPMP<sup>+</sup>-selective electrode in muscle mitochondria supplied with either  $18 \mu\text{M}$  PCarn, P/M (10/5 mM), or 9 mM succinate. Oxygen consumption was measured in parallel. Both  $\Psi\text{m}$  and  $\text{O}_2$  consumption were lower with a supply of  $18 \mu\text{M}$  PCarn as compared with saturating P/M or succinate (Fig. 3A). NAD(P)H/NAD(P)<sup>+</sup> autofluorescence also revealed a more reduced matrix environment with P/M than with PCarn oxidation (see supplemental Fig. 3C). Thus, a highly reduced ETC may not be required for FAO-induced ROS production.

To further characterize the relationship between  $\Psi\text{m}$  and ROS production during FAO,  $\Psi\text{m}$  was determined fluorimetrically over a range of [PCarn].  $\Psi\text{m}$  increased linearly with increasing [PCarn] from 0.5 to  $2.5 \mu\text{M}$  and then leveled off such that there was no change in  $\Psi\text{m}$  from 4.5 to  $18 \mu\text{M}$  PCarn (Fig. 3B), a range of [PCarn] over which the  $\text{H}_2\text{O}_2$  emission rate was found to increase (see Fig. 2A). Thus, PCarn-induced ROS production shows little  $\Psi\text{m}$ -dependence.

The  $\Psi\text{m}$  dependence of PCarn-induced ROS production was further explored in GSH-depleted mitochondria supplied with G/M (10/5 mM) or  $18 \mu\text{M}$  PCarn plus 2 mM L-carnitine (Fig. 3C). FCCP was used to titrate  $\Psi\text{m}$  in order to compare  $\text{H}_2\text{O}_2$  emission at different  $\Psi\text{m}$ . Depletion of GSH, using CDNB (49, 50), enabled significant ROS generation with oxidation of an NADH-linked substrate. L-Carnitine addition to mitochondria oxidizing PCarn results in higher  $\Psi\text{m}$  and  $\text{O}_2$  consumption (see below) and thus allowed comparison of  $\text{H}_2\text{O}_2$  emission over a wider range of  $\Psi\text{m}$  than could otherwise be achieved. As expected (12, 14), lowering  $\Psi\text{m}$  in mitochondria oxidizing G/M greatly decreased  $\text{H}_2\text{O}_2$  emission rate (by  $\sim 86\%$ ; Fig. 3C, circles). For a similar decrease in  $\Psi\text{m}$  from a similar higher value,

a decrease in  $\text{H}_2\text{O}_2$  emission was also apparent in mitochondria supplied with PCarn plus L-carnitine; however, the rate was decreased by only  $\sim 45\%$  (Fig. 3C, triangles). Thus, the  $\Psi\text{m}$  dependence of PCarn-induced ROS formation is substantially lower than for an NADH-linked substrate.

*Sites of Superoxide Production during PCarn Catabolism*—To further explore the mechanisms of ROS formation during FAO, we assessed whether superoxide was released on the matrix or the intermembrane space side of the inner membrane. Topology was determined using acetylated cytochrome *c* in the presence or absence of exogenous CuZn-superoxide dismutase (SOD) (51). Acetylated cytochrome *c* scavenges superoxide released into the intermembrane space, preventing its conversion to  $\text{H}_2\text{O}_2$  by endogenous CuZn-SOD localized to the intermembrane space. The SOD that is subsequently added competes with acetylated cytochrome *c* for superoxide. Accordingly, exogenous SOD becomes a more sensitive probe of intermembrane space superoxide.

With  $18 \mu\text{M}$  PCarn as substrate, the addition of 200 units/ml SOD approximately doubled the  $\text{H}_2\text{O}_2$  emission rate (Fig. 4A), indicating that some of the superoxide was released on the intermembrane space side of the inner membrane. Because some superoxide generated at complex III is released into the intermembrane space (13, 51), we determined whether complex III may be a site of superoxide formation during PCarn oxidation. To this end, we repeated the  $\text{H}_2\text{O}_2$  determinations with or without SOD in the presence of the complex III inhibitor antimycin ( $1 \mu\text{M}$ ) (Fig. 4B). Antimycin binds cytochrome *b* (52), increasing the steady state levels of ubiquinone at the ubiquinol binding site with subsequent superoxide formation (53). The addition of SOD yielded a quantitatively similar increase in  $\text{H}_2\text{O}_2$  emission rate in the presence as in the absence of antimycin (Fig. 4, compare A and B). This identifies complex

## Mechanisms of ROS Generation during LCFA Catabolism

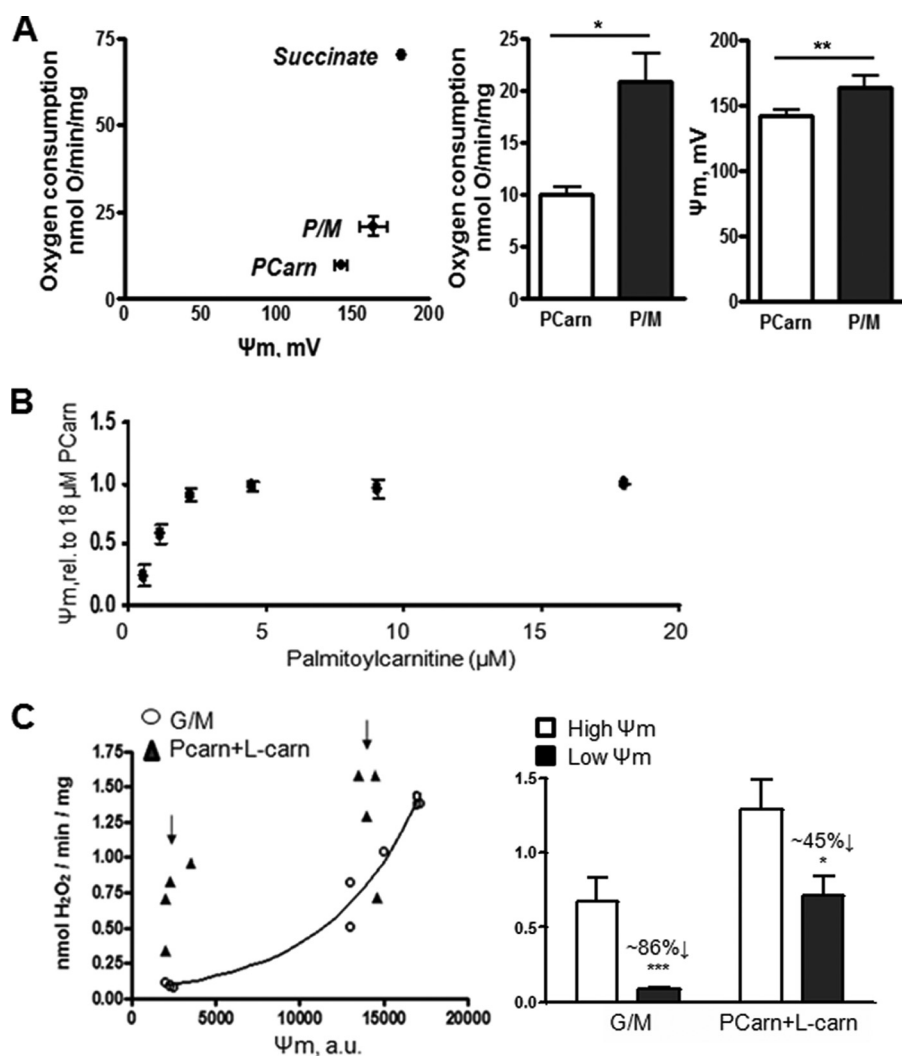


**FIGURE 3. Low energization of skeletal muscle mitochondria supplied with long-chain fatty acid substrate and relative insensitivity of H<sub>2</sub>O<sub>2</sub> to Ψ<sub>m</sub>.** *A*, parallel determinations of Ψ<sub>m</sub> and O<sub>2</sub> consumption in mitochondria respiring on 18 μM PCarn, 10/5 mM P/M, or 9 mM succinate (*n* = 2–5). Membrane potential was measured using a TPMP<sup>+</sup>-selective electrode. *Bar graphs*, statistical comparisons between PCarn and P/M. \* and \*\*, *p* < 0.03 and *p* < 0.01, respectively, paired *t* test. Values are means ± S.E. *B*, Ψ<sub>m</sub> determinations by safranin fluorescence. Values are means ± S.E., expressed as a fraction of the 18 μM PCarn value (*n* = 3). *C*, Ψ<sub>m</sub> and H<sub>2</sub>O<sub>2</sub> emission rate in skeletal muscle mitochondria supplied with 18 μM PCarn or G/M (10/5 mM). FCCP was used to titrate the membrane potential (PCarn, 15 μM FCCP; G/M, 100 μM FCCP). *Curve in C*, the Ψ<sub>m</sub>-H<sub>2</sub>O<sub>2</sub> relationship with G/M was fit using the equation,  $y = 0.06267e^{0.000183x}$  ( $R^2 = 0.988$ ). *Arrows in C*, values used for quantification in *bar graphs*. *Bar graphs*, average H<sub>2</sub>O<sub>2</sub> emission rates at Ψ<sub>m</sub> indicated by the arrows in *C* (*n* = 4). \* and \*\*\*, *p* < 0.05 or *p* < 0.005, respectively, paired *t* test, low versus high Ψ<sub>m</sub>. Values are means ± S.E. *Numbers above bars* summarize the approximate percentage decrease in H<sub>2</sub>O<sub>2</sub> emission rate when going from lower to higher membrane potential.

III as a possible site of superoxide formation during PCarn oxidation.

To further probe the sites of ROS generation during FAO, we compared H<sub>2</sub>O<sub>2</sub> emission rates in mitochondria supplied with 18 μM PCarn or P/M, in the presence of antimycin plus SOD or rotenone, which inhibits complex I (Fig. 4C). In the presence of rotenone, emission rates were 1.5–2 times higher with P/M than with PCarn. In contrast, emission rates in the presence of antimycin plus SOD were ~6 times greater with PCarn than with P/M. These observations with inhibitors further support the possibility that ROS formation at complex III contributes to the greater ROS generation during PCarn oxidation as compared with oxidation of NADH-linked substrates. However, contribution from upstream sites, such as the ETF and ETF-

QO, are also possible. The ETF is reduced by the dehydrogenases of β-oxidation, and it has been suggested that both the ETF and ETF-QO can exist in a partially reduced state (18). The fact that some of the ROS was released on the matrix side of the inner membrane and, significantly, that ROS is relatively Ψ<sub>m</sub>-independent support ROS formation at the ETF and ETF-QO.

It has been suggested that ROS generation during LCFA oxidation is due to backflow of electrons through complex I (*i.e.* RET) (13, 54). Distinct sites of complex I generate the ROS formed during rotenone inhibition and via RET (44). In addition, ROS generated by RET requires a high Ψ<sub>m</sub> (12, 48). We measured H<sub>2</sub>O<sub>2</sub> emission with succinate in the absence of inhibitors because this is known to generate ROS by RET (44). Rates measured with succinate (~0.8 nmol/min/mg) were lower than those with 18 μM PCarn in the presence of antimycin plus SOD (1.5–2 nmol/min/mg) (Fig. 4C). This observation together with the relatively low Ψ<sub>m</sub> generated during PCarn oxidation argue against backflow of electrons through complex I as an important ROS-generating process during PCarn oxidation.

*Fatty Acid Catabolic Intermediates Contribute to the ROS Load—*LCFA catabolic intermediates and by-products can inhibit the ETC (26–28) as well as the activity of several matrix enzymes whose activity can mitigate ROS formation (22–25). Thus, matrix levels of these

intermediates may be important determinants of the ROS load during PCarn oxidation. We tested this possibility by lowering the matrix level of catabolic intermediates using free L-carnitine (2 mM) (55–57). A subset of the intermediates formed during PCarn oxidation can be measured as <sup>14</sup>C recovered in the acid-soluble product ([<sup>14</sup>C]ASP) of a lipid extraction following oxidation of [1-<sup>14</sup>C]PCarn (32, 36). The [<sup>14</sup>C]ASP could thus include organic acids, acetyl-carnitine, and short and medium chain acylcarnitine species. Here, we used [<sup>14</sup>C]ASP as a measure of catabolic intermediate levels. To determine levels of intermediates associated with mitochondria or effluxed from mitochondria, subsequent to incubation with PCarn with or without L-carnitine, mitochondria were fractionated, and the [<sup>14</sup>C]ASP was measured in the pellet and buffer. To determine

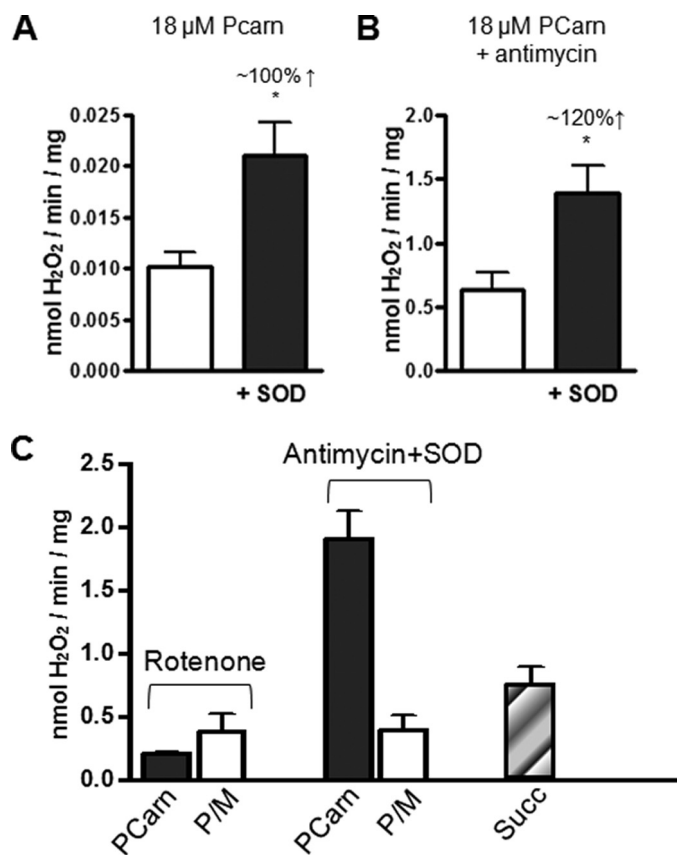


**FIGURE 4. Topology and sites of ROS production in skeletal muscle mitochondria oxidizing long-chain fatty acid substrate.** *A*,  $\text{H}_2\text{O}_2$  emission rate of mitochondria oxidizing 18  $\mu\text{M}$  PCarn in the absence or presence of added Cu/Zn-SOD (200 units/ml). *B*, as in *A*, with the addition of antimycin A (1  $\mu\text{M}$ ) to inhibit complex III. In *A* and *B*, the approximate percentage decrease increase in  $\text{H}_2\text{O}_2$  emission rate with SOD addition is given. Increased  $\text{H}_2\text{O}_2$  emission upon SOD addition indicates release of superoxide toward the intermembrane space. *C*, comparison of  $\text{H}_2\text{O}_2$  emission rates in mitochondria supplied with PCarn (18  $\mu\text{M}$ ) or P/M (10/5 mM), in the presence of rotenone (1  $\mu\text{M}$ ) to inhibit complex I or antimycin plus SOD. The  $\text{H}_2\text{O}_2$  emission rate was evaluated with a supply of succinate alone, which generates ROS by reverse electron transport to complex I. All values are means  $\pm$  S.E. ( $n = 3$ –5). \*,  $p < 0.03$ , paired *t* test, without SOD versus with SOD.

the generality of the L-carnitine effects, determinations were made in muscle and liver mitochondria.

In the absence of L-carnitine, the overall level (mitochondrial pellet plus buffer) of [ $^{14}\text{C}$ ]ASP was greater in liver than muscle mitochondria. Distribution of the [ $^{14}\text{C}$ ]ASP also differed between muscle and liver mitochondria (Fig. 5A). In muscle mitochondria,  $\sim 10\%$  was recovered in the pellet fraction, and  $\sim 90\%$  was recovered in the buffer fraction (*i.e.* was effluxed). In liver mitochondria, only 1.3% was recovered in the pellet. L-Carnitine increased the total recovered [ $^{14}\text{C}$ ]ASP in mitochondria (pellet plus buffer) from both muscle ( $p = 0.004$ ) and liver ( $p = 0.08$ ); an increase was detected in four of four preparations). Importantly, L-carnitine lead to a redistribution of the [ $^{14}\text{C}$ ]ASP from the pellet to the buffer fraction (Fig. 5A) in mitochondria from both tissues, with a greater shift in muscle mitochondria.  $^{14}\text{CO}_2$  production was low under the non-phosphorylating conditions of the experiments ( $\sim 3$  and 1 nmol of  $\text{CO}_2$ /h/mg in muscle and liver mitochondria, respectively) and was slightly lowered by L-carnitine in mitochondria from both tissues (Fig. 5B). These changes in [ $^{14}\text{C}$ ]ASP distribution with

L-carnitine addition are consistent with a decrease in the level of intermediates within the matrix of muscle and liver mitochondria.

Although our observations indicate that ROS is less sensitive to the ETC redox state when LCFA are oxidized, some  $\Psi_m$  sensitivity remained (see Fig. 3C). Thus, to provide context for the interpretation of the  $\text{H}_2\text{O}_2$  data, changes in bioenergetic parameters with L-carnitine are presented first. L-Carnitine addition to muscle mitochondria catabolizing 18  $\mu\text{M}$  PCarn led to greater membrane polarization, greater  $\text{O}_2$  consumption, and increased NAD(P)H/NAD(P) $^+$  (Fig. 5, C and D, and supplemental Fig. 2). No such changes were observed with L-carnitine in liver mitochondria (Fig. 5, C and D, and supplemental Fig. 2). The findings in muscle mitochondria with or without carnitine are consistent with higher ETC flux enabled by a decrease in an inhibitory intermediate(s). The fact that  $^{14}\text{CO}_2$  production did not increase in muscle mitochondria (but instead decreased) argues against the possibility that higher  $\text{O}_2$  consumption and  $\Psi_m$  reflect greater availability of PCarn for catabolism due to facilitation of its uptake by L-carnitine. The specificity of L-carnitine for the reactions of  $\beta$ -oxidation was confirmed by the absence of L-carnitine effects on  $\text{O}_2$  consumption,  $\Psi_m$ , and NAD(P)H/NAD(P) $^+$  of muscle mitochondria supplied with P/M or G/M (supplemental Fig. 3).

To test the possible effects of catabolic intermediates on ROS production, we next determined the  $\text{H}_2\text{O}_2$  emission rate in the absence and presence of L-carnitine. In muscle mitochondria, the addition of L-carnitine resulted in minimal changes in  $\text{H}_2\text{O}_2$  emission rate, whereas the  $\text{H}_2\text{O}_2$  emission rate was lowered in liver mitochondria (Fig. 5E). These observations support the hypothesis that catabolic intermediates contribute to ROS production in liver mitochondria. The interpretation of the  $\text{H}_2\text{O}_2$  data in muscle mitochondria is complicated by the L-carnitine-induced increase in  $\text{O}_2$  consumption and  $\Psi_m$ . On the one hand, these increases would predict greater ROS generation (see Fig. 3C) (12, 14). However, we have observed that PCarn-induced  $\text{H}_2\text{O}_2$  emission is less dependent on  $\Psi_m$  as compared with an NADH-linked substrate (Fig. 3C). Thus, the absence of a change in  $\text{H}_2\text{O}_2$  emission with L-carnitine could simply indicate that LCFA catabolic intermediates have little effect on ROS in muscle mitochondria.

To further investigate the role of LCFA catabolic intermediates in ROS production, we determined whether the glutathione antioxidant system was impeded. CDNB was used to deplete GSH in muscle and liver mitochondria (49, 50). If L-carnitine increases the capacity of the glutathione antioxidant system (by relieving inhibition by catabolic intermediates), then the addition of L-carnitine to GSH-depleted mitochondria should produce a relative increase in  $\text{H}_2\text{O}_2$  emission compared with that measured in carnitine-treated mitochondria with normal GSH levels. Predictably, GSH depletion greatly ( $\sim 10$  fold) increased  $\text{H}_2\text{O}_2$  emission in mitochondria from both muscle and liver. In GSH-depleted liver mitochondria, the addition of L-carnitine still lowered the  $\text{H}_2\text{O}_2$  emission rate, by  $\sim 50\%$  (Fig. 5F). It is not clear that the L-carnitine addition to GSH-depleted liver mitochondria produced less of a decrease in  $\text{H}_2\text{O}_2$  emission compared with that measured in GSH-intact mitochondria. Thus, although higher levels of LCFA catabolic

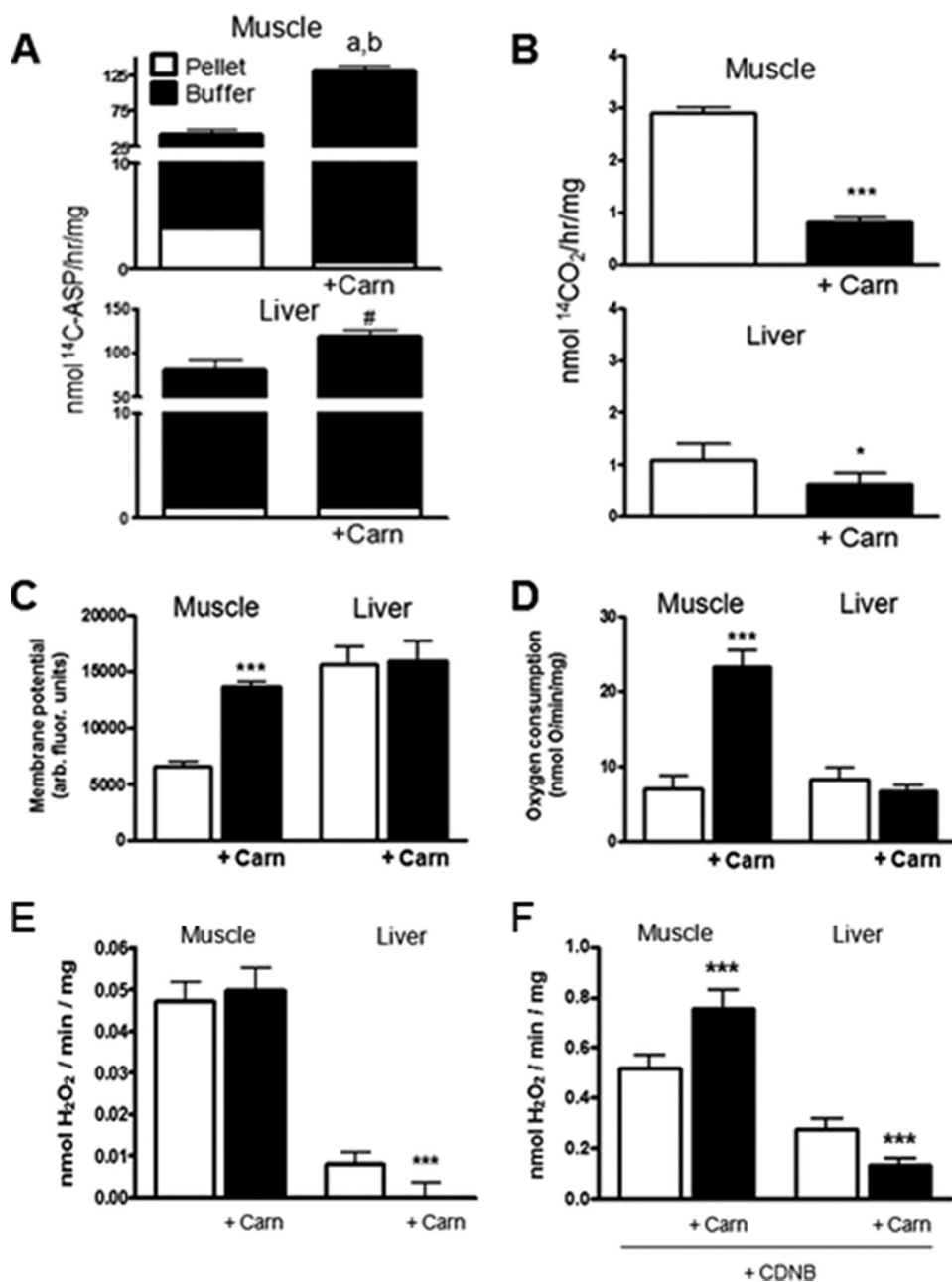


**FIGURE 5. L-Carnitine effects on bioenergetics and  $\text{H}_2\text{O}_2$  emission rates of skeletal muscle and liver mitochondria.** L-Carnitine (2 mM; *Carn*) was utilized to decrease levels of long-chain fatty acid catabolic intermediates within the mitochondrial matrix. Mitochondria (0.2 mg/ml) were supplied with 18  $\mu\text{M}$  PCarn. **A**, in mitochondria supplied with PCarn plus [ $^{14}\text{C}$ ]palmitoylcarnitine, the [ $^{14}\text{C}$ ]acid-soluble product ( $^{14}\text{C}$ -ASP) was used as a measure of LCFA catabolic intermediate levels within the matrix (*pellet*) and effluxed from mitochondria into the buffer (*buffer*). Above the bar in the muscle panel, *a* and *b*,  $p < 0.003$  and  $p < 0.015$  for buffer and pellet fractions, respectively, paired *t* test, without L-carnitine versus with L-carnitine. Above the bar in the liver panel, #,  $p = 0.08$ , paired *t* test, [ $^{14}\text{C}$ ]ASP was increased in the buffer fraction in four of four preparations. **B**, rate of  $^{14}\text{CO}_2$  production. **C–F**, bioenergetic parameters (**C** and **D**) and  $\text{H}_2\text{O}_2$  emission rates (**E** and **F**) were determined under the same conditions as in **A** and **B**, using only cold PCarn. In **F**, CDNB was used to deplete mitochondria of reduced glutathione. **A–D**,  $n = 4$ ; **E** and **F**,  $n = 7–8$ . In all panels, values are means  $\pm$  S.E. \* and \*\*\*,  $p < 0.05$  and  $p < 0.005$ , respectively, paired *t* test.

intermediates are associated with greater ROS in liver mitochondria, this may not be due to interference of GSH antioxidant pathways.

In contrast to what was observed in liver mitochondria, as well as to what was observed with an intact glutathione antioxidant system, L-carnitine increased the  $\text{H}_2\text{O}_2$  emission rate by ~40% in GSH-depleted muscle mitochondria (Fig. 6B).

These observations are consistent with an increase in the capacity of the glutathione antioxidant system in muscle mitochondria upon the addition of L-carnitine and thus support a role for LCFA catabolic intermediates in ROS production in muscle mitochondria.

CDNB had a slight uncoupling effect in both muscle and liver mitochondria (supplemental Fig. 4, muscle mitochondria and liver mitochondria) (data not shown), the extent of which was similar with or without L-carnitine (not shown). Thus, while it is generally accepted that uncoupling mitigates ROS production, the effect of any uncoupling on  $\text{H}_2\text{O}_2$  emission would be similar in liver mitochondria with or without L-carnitine because L-carnitine had no effect on  $\Psi_m$ . Because L-carnitine increased  $\Psi_m$  in muscle mitochondria, the increase in the  $\text{H}_2\text{O}_2$  emission rate with the L-carnitine addition may be slightly underestimated (by 0–15%, estimated using the  $\Psi_m$ - $\text{H}_2\text{O}_2$  relationship for PCarn plus L-carnitine from the data in Fig. 3C).

**NNT (Nicotinamide Nucleotide Transhydrogenase) Activity Is Not Impeded during LCFA Catabolism**—We had initially thought that higher ROS in mitochondria oxidizing PCarn might be due to a diminished ability to regenerate NADPH via NNT. NNT is localized to the mitochondrial inner membrane, where it catalyzes the transfer of a hydride ion from NADH to  $\text{NADP}^+$  coupled to  $\text{H}^+$  transport into the matrix. NNT is considered to be a significant source of mitochondrial NADPH required for regeneration of GSH from its oxidized form (58). We hypothesized that NNT activity might be decreased, due either to the relatively low state of membrane energization during PCarn catabolism (Fig. 3A) or to inhibition by acyl-CoA species (24). However, C57Bl/6J mice can harbor a spontaneous five-exon deletion in the *Nnt* gene, which is associated with undetectable levels of enzyme activity and protein (59–61). Genotyping of our mice, originally from Jackson Laboratories, revealed that they carried this deletion (supplemental Fig. 5). Thus, inhibition of NNT activity cannot be the cause of L-carnitine effects on  $\text{H}_2\text{O}_2$  emission.

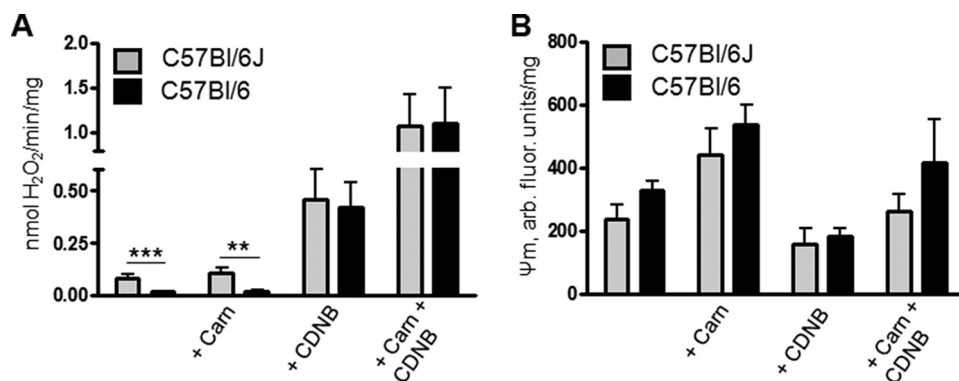


**FIGURE 6. Impact of NNT deletion on carnitine effects on H<sub>2</sub>O<sub>2</sub> emission in skeletal mitochondria from C57Bl/6J and C57Bl/6 mice.** Mitochondria were supplied with 18  $\mu$ M palmitoylcarnitine. *A*, H<sub>2</sub>O<sub>2</sub> emission rates. *B*,  $\Psi_m$ . C57Bl/6J mice harbor a five-exon deletion in the *Nnt* gene (see supplemental Fig. 5). *Nnt* encodes for NNT, which is thought to be largely responsible for NAD(P)H regeneration in mitochondria and thus to contribute to the maintenance of glutathione antioxidant defense. Values are means  $\pm$  S.E.,  $n = 3$ . \*\* and \*\*\*,  $p < 0.03$  and  $p < 0.01$ , respectively, without carnitine versus with carnitine, two-way analysis of variance with Bonferroni *post hoc* tests.

Because of the reported inhibitory effect of acyl-CoA species on NNT activity (24), we wanted to test whether this inhibition would impact ROS production in mitochondria oxidizing PCarn. We compared H<sub>2</sub>O<sub>2</sub> emission rates in muscle mitochondria from C57Bl/6J mice and from C57Bl/6 mice from Charles River, which do not carry the NNT mutation (supplemental Fig. 5). L-Carnitine was used to lower the level of matrix catabolic intermediates. If LCFA catabolic intermediates inhibit NNT, then the effect of L-carnitine on H<sub>2</sub>O<sub>2</sub> emission should be greater in mitochondria from C57Bl/6 mice. In mitochondria oxidizing 18  $\mu$ M PCarn, H<sub>2</sub>O<sub>2</sub> emission was lower in C57Bl/6 than in C57Bl/6J mitochondria (Fig. 6A). Moreover, GSH depletion increased H<sub>2</sub>O<sub>2</sub> emission more in C57Bl/6 than in C57Bl/6J mitochondria (Fig. 6A). The latter observations are consistent with a role for NNT in mitigating ROS production in muscle mitochondria. However, L-carnitine had quantitatively similar effects on H<sub>2</sub>O<sub>2</sub> emission and on  $\Psi_m$  in C57Bl/6 and C57Bl/6J mitochondria (Fig. 6, A and B). Thus, despite the ability of acyl-CoAs to inhibit NNT (24), such inhibition probably does not play an important role in ROS formation during PCarn catabolism.

## DISCUSSION

In this study, we aimed 1) to determine whether lower, more physiologic [LCFA] is associated with higher rates of ROS formation than NADH-linked substrates and 2) to obtain insight into mechanisms underlying ROS formation during LCFA catabolism (see Fig. 1). We have made the novel observations that ROS formation during LCFA catabolism can occur at low [LCFA], can be substantial even when the inner membrane is relatively depolarized, and exhibits relatively low dependence on  $\Psi_m$ . ROS generation at the ETF and/or ETF-QO is a possible  $\Psi_m$ -independent mechanism. Our observations also indicate that PCarn-induced ROS is generated at complex III, whereas generation at complex I may be less important. Finally, we have also identified a novel link between H<sub>2</sub>O<sub>2</sub> emission and levels of LCFA intermediates in muscle and liver mitochondria.

Rotenone and antimycin are commonly used to investigate the mechanisms of ROS production in mitochondria

(e.g. see Refs. 13, 17, and 34). At saturating concentrations, these inhibitors maximally reduce complexes I and III as well as upstream redox centers. The superoxide that is formed reflects the capability of these sites to generate ROS but does not necessarily indicate whether generation at these sites occurs under physiologic conditions. In this study, we minimized the use of these inhibitors and integrated results from such determinations with those from several complementary approaches (increasing [PCarn], with or without L-carnitine, CDNB, and NNT) to provide a more comprehensive view of the possible mechanisms of ROS production.

**Relationship of H<sub>2</sub>O<sub>2</sub> Emission with  $\Psi_m$** —Our findings demonstrate that the catabolism of even low [LCFA] induces a significant rate of H<sub>2</sub>O<sub>2</sub> emission, whereas saturating concentrations of NADH-linked substrates yield no discernable rates. Yet, the highest H<sub>2</sub>O<sub>2</sub> emission rate with PCarn was associated with  $\Psi_m$  that was lower than  $\Psi_m$  generated by P/M, G/M, or succinate. Our finding of relatively lower  $\Psi_m$  (~145 mV) during PCarn oxidation qualitatively and quantitatively corroborates recent findings in rat skeletal muscle mitochondria oxidizing FA and non-FA substrates under state 4 conditions (34). These results support the notion that PCarn catabolism is associated with significant ROS production that is not due to a relatively more reduced state of the ETC. In addition, whereas  $\Psi_m$  leveled off at 4.5  $\mu$ M PCarn, the H<sub>2</sub>O<sub>2</sub> emission rate continued to rise with [PCarn] up to 18  $\mu$ M (see Figs. 2A and 3B). Moreover, lower  $\Psi_m$  dependence was measured with PCarn plus L-carnitine compared with G/M in GSH-depleted mitochondria (Fig. 3C). Altogether, these findings suggest that ETC redox state is not the only or possibly even the main determinant of ROS formation during FAO. A  $\Psi_m$ -independent component of ROS formation was also observed in brain mitochondria (15–17). The present study is, to our knowledge, the first to report this phenomenon in muscle mitochondria.

**$\Psi_m$ -independent Mechanisms of H<sub>2</sub>O<sub>2</sub> Emission during PCarn Catabolism**—Possible  $\Psi_m$ -independent mechanisms of H<sub>2</sub>O<sub>2</sub> emission during FAO can be categorized as those that generate ROS and those that inhibit detoxifying mechanisms. Strong candidates for the former are the ETF and ETF-QO. Specifically, we propose that ETC inhibition by LCFA intermediates leads to increased escape of electrons from the ETF and/or ETF-QO. This proposal is based on the following. First, experiments conducted in the presence of rotenone and antimycin indicate a role for complex III and upstream sites in superoxide generation (e.g. ETF and ETF-QO (18)). Second,  $\Psi_m$  did not increase further for [PCarn] > 4.5  $\mu$ M, whereas H<sub>2</sub>O<sub>2</sub> emission continued to rise with higher [PCarn], suggesting that  $\beta$ -oxidation continued despite inhibited ETC flux. Finally, we have found that ROS generated during FAO is relatively insensitive to  $\Psi_m$ . A direct test of the contribution from



## Mechanisms of ROS Generation during LCFA Catabolism

the ETF and ETF-QO to ROS production is complicated by the lack of reagents to specifically study these enzymes. St-Pierre *et al.* (13) proposed the ETF and ETF-QO as sites for ROS production based on differential H<sub>2</sub>O<sub>2</sub> emission in the presence of rotenone or antimycin. The present study integrates evidence obtained using inhibitors with information about ETC redox state and thus provides stronger evidence for a role for the ETF and/or ETF-QO in ROS production.

Mitochondrial enzymes that directly or indirectly mitigate ROS formation can be modified by LCFA catabolic intermediates or by-products. Specifically, NNT and ANT activity can be inhibited by acyl-CoA species (22–24), and NADP<sup>+</sup>-linked isocitrate dehydrogenase is partially inactivated by 4-hydroxynonenal (25). These observations suggest that intermediates of LCFA catabolism would modulate ROS formation. We used L-carnitine to lower the matrix level of catabolic intermediates; indeed, L-carnitine addition was associated with increased recovery of [<sup>14</sup>C]ASP in the buffer fraction of both muscle and liver mitochondria. L-carnitine is well known as a requirement for LCFA-CoA uptake into mitochondria by carnitine palmitoyltransferase-1. A less appreciated role for carnitine is in the regulation of matrix acyl-CoA/CoA by exchange of cytosolic carnitine with matrix acylcarnitine, catalyzed by carnitine acylcarnitine transferase (62) (see Fig. 1). Previous studies have established that L-carnitine added to suspensions of skeletal muscle, cardiac, or liver mitochondria leads to efflux of acetyl-carnitine and longer chain acylcarnitine species (55–57). This efflux occurs with minimal or no change in complete oxidation to CO<sub>2</sub> (36). L-Carnitine clearly lowered the H<sub>2</sub>O<sub>2</sub> emission rate in liver mitochondria, and this occurred in the absence of bioenergetic changes. The fact that L-carnitine addition to muscle mitochondria increased Ψ<sub>m</sub> and O<sub>2</sub> consumption complicates the interpretation of the L-carnitine effect on H<sub>2</sub>O<sub>2</sub> emission rate. However, that L-carnitine increased H<sub>2</sub>O<sub>2</sub> emission in GSH-depleted mitochondria but had little effect in intact mitochondria supports a role for intermediates/by-products of LCFA catabolism in determining ROS levels in muscle mitochondria. It is also noteworthy that H<sub>2</sub>O<sub>2</sub> emission/O<sub>2</sub> consumed was lower in the presence compared with the absence of L-carnitine in muscle (no GSH depletion) and liver mitochondria. Thus, our observations support a model in which L-carnitine buffers the matrix levels of LCFA catabolic intermediates, thereby decreasing the ROS associated with LCFA catabolism. Our findings may in part explain observations that *in vivo* administration of L-carnitine lowers oxidative stress in cardiac muscle (63, 64). Since insulin resistance has been linked to oxidative stress (4, 5), our findings may also explain the improved insulin-mediated glucose disposal in mice supplemented with L-carnitine (65–67).

Experiments with GSH-depleted mitochondria suggest that some component(s) of the glutathione antioxidant system of muscle mitochondria are inhibited during LCFA catabolism, such that L-carnitine addition leads to an expanded functional capacity of this system. Our results, however, rule out NNT inhibition as an underlying mechanism. Differently from muscle mitochondria, GSH depletion of liver mitochondria had little impact on the effect of L-carnitine to lower H<sub>2</sub>O<sub>2</sub> emission. It is likely that the profile of accumulated metabolites differs in

muscle and liver mitochondria during PCarn catabolism, such that a decrease in matrix intermediates impacts matrix pathways differently in mitochondria from the two tissues.

Interestingly, the L-carnitine-induced redistribution of [<sup>14</sup>C]ASP from pellet to buffer was more pronounced in muscle than in liver mitochondria. In fact, in the absence of L-carnitine, recovery of [<sup>14</sup>C]ASP in the buffer fraction was higher in liver than muscle mitochondria, suggesting that accumulation of intermediates is lower in the former. L-Carnitine also had a profound effect on O<sub>2</sub> consumption and Ψ<sub>m</sub> of muscle but not liver mitochondria. It is also noteworthy that state 3 and 4 respiration rates with PCarn were similar in liver and muscle mitochondria (supplemental Table 1). Collectively, these observations suggest that an important difference between liver and muscle mitochondria oxidizing LCFA is how intermediates are handled. This difference could reflect higher flux through carnitine acyltransferase and carnitine acylcarnitine transferase in liver mitochondria and could contribute to the lower PCarn-induced ROS in liver compared with muscle mitochondria.

Peroxisomes also catabolize LCFA, especially in hepatocytes (68), and peroxisomal catabolism of acyl-CoA species can yield significant H<sub>2</sub>O<sub>2</sub> (69). However, peroxisomal β-oxidation probably does not explain our observations because PCarn (as opposed to palmitate or palmitoyl-CoA) was the substrate used in these studies. Uptake into peroxisomes of PCarn seems unlikely despite peroxisomal expression of carnitine acyltransferases, because mouse carnitine acyltransferase has no activity for ≥C16 substrates (70).

*Topology of ROS Production and Role of the ETC*—Our finding that ROS formed during FAO can be released on the intermembrane space side of the mitochondrial inner membrane differs from that of St-Pierre *et al.* (13), who observed similar H<sub>2</sub>O<sub>2</sub> emission rates with the addition of SOD to muscle mitochondria oxidizing 60 μM PCarn under state 4 conditions. It is likely that use of acetylated cytochrome *c* in the present study created a more sensitive detection system. Another explanation for the discrepant findings is the use of higher [PCarn] by St-Pierre *et al.* (13), which could have led to greater ETC inhibition. Increased H<sub>2</sub>O<sub>2</sub> generation with SOD addition has been attributed to superoxide formation at the ubiquinol binding site of complex III and its subsequent release into the intermembrane space (13, 51). Another potential source of superoxide in the intermembrane space is p66<sup>shc</sup>, which possesses oxidoreductase activity and can specifically oxidize cytochrome *c* (71). However, the fact that the extent of the increase with an SOD addition was similar in the presence and absence of complex III inhibition points to complex III as a source of ROS during FAO.

Observations presented in Fig. 4 do not support complex I, via forward or reverse electron flow, as an important site for ROS production during FAO, in contrast to earlier suggestions (13, 54). Reverse electron flow is supported by a high Ψ<sub>m</sub> (12, 48). The relatively depolarized Ψ<sub>m</sub> of mitochondria oxidizing PCarn provides an additional argument against ROS generation by RET.

Fatty acids and lipid peroxidation products, such as 4-hydroxynonenal, can activate uncoupling mechanisms mediated by ANT and UCP3 (*e.g.* see Refs. 72 and 73), leading to lower

ROS formation. In support, in a study in preparation, we have found that ANT is activated with oxidation of 18  $\mu\text{M}$  PCarn, thereby lowering  $\text{H}_2\text{O}_2$  emission; the effect of ANT activation on  $\text{H}_2\text{O}_2$  was similar at higher and lower  $\Psi\text{m}$ . UCP3 was also activated, thereby lowering  $\text{H}_2\text{O}_2$  emission; like ANT, the effect of UCP3 was similar at higher and lower  $\Psi\text{m}$ . Notably, it is despite the activation of ANT and UCP3 that PCarn oxidation is associated with greater ROS formation. Because acyl-CoA species can inhibit ANT (23), we also evaluated this possibility and found it to be unlikely.

**Study Limitations**—The ASP fraction is a heterogeneous mixture probably containing acetyl-carnitine and short- and medium-chain acylcarnitines (55–57), small organic acids, and also, in liver mitochondria, ketone bodies. However, the present study leaves open the questions of the precise composition of the ASP, particularly the differences between muscle and liver mitochondria, and of how LCFA intermediates are linked to ROS production. Thus, further investigation in this regard is warranted.

Tools to reliably address *in vivo* mitochondrial ROS production are currently lacking (54). Thus, isolated mitochondria remain the best system for detailed mechanistic studies of mitochondrial ROS production, the focus of this study. However, extrapolation of observations from isolated mitochondria to the *in vivo* context cannot be made accurately (54). Nevertheless, several studies have demonstrated a role for mitochondrially derived  $\text{H}_2\text{O}_2$ , in the absence of ETC inhibitors, in mediating cell function under steady state conditions, including in whole animals in which FAO is higher during the rest phase of the day (8–10). Thus, it seems reasonable to infer that the low rates of mitochondrial  $\text{H}_2\text{O}_2$  emission during PCarn oxidation that we report here could impact steady state cell function.

**Implications**—The present study, along with others (4, 11), demonstrates the capacity of LCFA to generate significant mitochondrial ROS. Here we have shown that this capacity is not confined to a narrow operational state of mitochondria, namely high  $\Psi\text{m}$ , or to an elevated supply of LCFA. Rather, it is expressed across the physiologic span of  $\Psi\text{m}$  and with low LCFA supply, indicating a wide functional range over which FAO-induced ROS can impact processes within mitochondria and in other cellular compartments. Our finding that ROS are released not only on the matrix side but also on the cytosolic side of the inner membrane broadens the spatial range over which FAO-induced ROS can have an impact on mitochondrial and extramitochondrial processes. The fact that LCFA intermediates play an important role in determining the ROS burden indicates that selective up-regulation of mechanisms that enhance mitochondrial LCFA uptake and  $\beta$ -oxidation may be associated with increased ROS formation. Conversely, up-regulation of mechanisms that increase the clearance of LCFA intermediates from mitochondria should lower the ROS load. More generally, our observations suggest that the existence of processes to buffer the levels of LCFA catabolic intermediates confers cellular protection from excessive mitochondrial ROS generation with increased provisioning of LCFA substrate as would occur with exercise, fasting, or insulin resistance.

**Acknowledgments**—We are grateful to the members of the Harper laboratory for discussions and comments related to the manuscript. We also thank the three anonymous reviewers for the many constructive comments that greatly improved the manuscript.

## REFERENCES

- Hansford, R. G., Hogue, B. A., and Mildaziene, V. (1997) *J. Bioenerg. Biomembr.* **29**, 89–95
- Chance, B., Sies, H., and Boveris, A. (1979) *Physiol. Rev.* **59**, 527–605
- Abdul-Ghani, M. A., Jani, R., Chavez, A., Molina-Carrion, M., Tripathy, D., and DeFronzo, R. A. (2009) *Diabetologia* **52**, 574–582
- Anderson, E. J., Lustig, M. E., Boyle, K. E., Woodlief, T. L., Kane, D. A., Lin, C. T., Price, J. W., 3rd, Kang, L., Rabinovitch, P. S., Szeto, H. H., Houmar, J. A., Cortright, R. N., Wasserman, D. H., and Neuffer, P. D. (2009) *J. Clin. Invest.* **119**, 573–581
- Bonnard, C., Durand, A., Peyrol, S., Chanseume, E., Chauvin, M. A., Morio, B., Vidal, H., and Rieusset, J. (2008) *J. Clin. Invest.* **118**, 789–800
- Jackson, M. J. (2008) *Free Radic. Biol. Med.* **44**, 132–141
- Davidson, S. M., and Duchon, M. R. (2007) *Circ. Res.* **100**, 1128–1141
- Houstis, N., Rosen, E. D., and Lander, E. S. (2006) *Nature* **440**, 944–948
- Hoehn, K. L., Salmon, A. B., Hohnen-Behrens, C., Turner, N., Hoy, A. J., Maghazal, G. J., Stocker, R., Van Remmen, H., Kraegen, E. W., Cooney, G. J., Richardson, A. R., and James, D. E. (2009) *Proc. Natl. Acad. Sci. U.S.A.* **106**, 17787–17792
- Loh, K., Deng, H., Fukushima, A., Cai, X., Boivin, B., Galic, S., Bruce, C., Shields, B. J., Skiba, B., Ooms, L. M., Stepto, N., Wu, B., Mitchell, C. A., Tonks, N. K., Watt, M. J., Febrario, M. A., Crack, P. J., Andrikopoulos, S., and Tiganis, T. (2009) *Cell Metab.* **10**, 260–272
- Chen, Q., Vazquez, E. J., Moghaddas, S., Hoppel, C. L., and Lesnfsky, E. J. (2003) *J. Biol. Chem.* **278**, 36027–36031
- Liu, Y., Fiskum, G., and Schubert, D. (2002) *J. Neurochem.* **80**, 780–787
- St-Pierre, J., Buckingham, J. A., Roeback, S. J., and Brand, M. D. (2002) *J. Biol. Chem.* **277**, 44784–44790
- Korshunov, S. S., Skulachev, V. P., and Starkov, A. A. (1997) *FEBS Lett.* **416**, 15–18
- Votyakova, T. V., and Reynolds, I. J. (2001) *J. Neurochem.* **79**, 266–277
- Sipos, L., Tretter, L., and Adam-Vizi, V. (2003) *Neurochem. Res.* **28**, 1575–1581
- Tretter, L., and Adam-Vizi, V. (2007) *Neurochem. Res.* **32**, 569–575
- Ramsay, R. R., Steenkamp, D. J., and Husain, M. (1987) *Biochem. J.* **241**, 883–892
- Starkov, A. A., Fiskum, G., Chinopoulos, C., Lorenzo, B. J., Browne, S. E., Patel, M. S., and Beal, M. F. (2004) *J. Neurosci.* **24**, 7779–7788
- Chinopoulos, C., Tretter, L., and Adam-Vizi, V. (2000) *Neurochem. Int.* **36**, 483–488
- Tretter, L., and Adam-Vizi, V. (2004) *J. Neurosci.* **24**, 7771–7778
- Ciapaite, J., Van Eikenhorst, G., Bakker, S. J., Diamant, M., Heine, R. J., Wagner, M. J., Westerhoff, H. V., and Krab, K. (2005) *Diabetes* **54**, 944–951
- Woldegiorgis, G., Yousufzai, S. Y., and Shrago, E. (1982) *J. Biol. Chem.* **257**, 14783–14787
- Rydström, J. (1972) *Eur. J. Biochem.* **31**, 496–504
- Benderdour, M., Charron, G., DeBlois, D., Comte, B., and Des Rosiers, C. (2003) *J. Biol. Chem.* **278**, 45154–45159
- Abdul-Ghani, M. A., Muller, F. L., Liu, Y., Chavez, A. O., Balas, B., Zuo, P., Chang, Z., Tripathy, D., Jani, R., Molina-Carrion, M., Monroy, A., Folli, F., Van Remmen, H., and DeFronzo, R. A. (2008) *Am. J. Physiol. Endocrinol. Metab.* **295**, E678–E685
- Sauer, S. W., Okun, J. G., Hoffmann, G. F., Koelker, S., and Morath, M. A. (2008) *Biochim. Biophys. Acta* **1777**, 1276–1282
- Guduz, T. I., Tserng, K. Y., and Hoppel, C. L. (1997) *J. Biol. Chem.* **272**, 24154–24158
- Adams, S. H., Hoppel, C. L., Lok, K. H., Zhao, L., Wong, S. W., Minkler, P. E., Hwang, D. H., Newman, J. W., and Garvey, W. T. (2009) *J. Nutr.* **139**, 1073–1081
- Wensaas, A. J., Rustan, A. C., Just, M., Berge, R. K., Drevon, C. A., and

## Mechanisms of ROS Generation during LCFA Catabolism

- Gaster, M. (2009) *Diabetes* **58**, 527–535
31. Hancock, C. R., Han, D. H., Chen, M., Terada, S., Yasuda, T., Wright, D. C., and Holloszy, J. O. (2008) *Proc. Natl. Acad. Sci. U.S.A.* **105**, 7815–7820
32. Koves, T. R., Ussher, J. R., Noland, R. C., Slentz, D., Mosedale, M., Ilkayeva, O., Bain, J., Stevens, R., Dyck, J. R., Newgard, C. B., Lopaschuk, G. D., and Muoio, D. M. (2008) *Cell Metab.* **7**, 45–56
33. Turner, N., Bruce, C. R., Beale, S. M., Hoehn, K. L., So, T., Rolph, M. S., and Cooney, G. J. (2007) *Diabetes* **56**, 2085–2092
34. Tahara, E. B., Navarete, F. D., and Kowaltowski, A. J. (2009) *Free Radic. Biol. Med.* **46**, 1283–1297
35. Chappell, J. B., and Perry, S. V. (1954) *Nature* **173**, 1094–1095
36. Seifert, E. L., Bézaire, V., Estey, C., and Harper, M. E. (2008) *J. Biol. Chem.* **283**, 25124–25131
37. Boily, G., Seifert, E. L., Bevilacqua, L., He, X. H., Sabourin, G., Estey, C., Moffat, C., Crawford, S., Saliba, S., Jardine, K., Xuan, J., Evans, M., Harper, M. E., and McBurney, M. W. (2008) *PLoS ONE* **3**, e1759
38. Hoffman, D. L., and Brookes, P. S. (2009) *J. Biol. Chem.* **284**, 16236–16245
39. Hyslop, P. A., and Sklar, L. A. (1984) *Anal. Biochem.* **141**, 280–286
40. Bhattacharya, A., Muller, F. L., Liu, Y., Sabia, M., Liang, H., Song, W., Jang, Y. C., Ran, Q., and Van Remmen, H. (2009) *J. Biol. Chem.* **284**, 46–55
41. Reynafarje, B., Costa, L. E., and Lehninger, A. L. (1985) *Anal. Biochem.* **145**, 406–418
42. Brown, G. C., and Cooper, C. E. (eds) (2002) *Bioenergetics: A Practical Approach*, pp. 49–62, Oxford University Press, Oxford
43. Akerman, K. E., and Wikström, M. K. (1976) *FEBS Lett.* **68**, 191–197
44. Lambert, A. J., Buckingham, J. A., and Brand, M. D. (2008) *FEBS Lett.* **582**, 1711–1714
45. Penzo, D., Tagliapietra, C., Colonna, R., Petronilli, V., and Bernardi, P. (2002) *Biochim. Biophys. Acta* **1555**, 160–165
46. Wieckowski, M. R., Brdiczka, D., and Wojtczak, L. (2000) *FEBS Lett.* **484**, 61–64
47. Shabalina, I. G., Kramarova, T. V., Nedergaard, J., and Cannon, B. (2006) *Biochem. J.* **399**, 405–414
48. Kushnareva, Y., Murphy, A. N., and Andreyev, A. (2002) *Biochem. J.* **368**, 545–553
49. Schönfeld, P., and Wojtczak, L. (2007) *Biochim. Biophys. Acta* **1767**, 1032–1040
50. Jocelyn, P. C., and Cronshaw, A. (1985) *Biochem. Pharmacol.* **34**, 1588–1590
51. Muller, F. L., Liu, Y., and Van Remmen, H. (2004) *J. Biol. Chem.* **279**, 49064–49073
52. Zhang, Z., Huang, L., Shulmeister, V. M., Chi, Y. I., Kim, K. K., Hung, L. W., Crofts, A. R., Berry, E. A., and Kim, S. H. (1998) *Nature* **392**, 677–684
53. Turrens, J. F. (2003) *J. Physiol.* **552**, 335–344
54. Murphy, M. P. (2009) *Biochem. J.* **417**, 1–13
55. Lysiak, W., Lilly, K., DiLisa, F., Toth, P. P., and Bieber, L. L. (1988) *J. Biol. Chem.* **263**, 1151–1156
56. Brass, E. P., and Hoppel, C. L. (1980) *Biochem. J.* **188**, 451–458
57. Stanley, K. K., and Tubbs, P. K. (1975) *Biochem. J.* **150**, 77–88
58. Pedersen, A., Karlsson, G. B., and Rydström, J. (2008) *J. Bioenerg. Biomembr.* **40**, 463–473
59. Huang, T. T., Naemuddin, M., Elchuri, S., Yamaguchi, M., Kozy, H. M., Carlson, E. J., and Epstein, C. J. (2006) *Hum. Mol. Genet.* **15**, 1187–1194
60. Freeman, H., Shimomura, K., Horner, E., Cox, R. D., and Ashcroft, F. M. (2006) *Cell Metab.* **3**, 35–45
61. Freeman, H. C., Hugill, A., Dear, N. T., Ashcroft, F. M., and Cox, R. D. (2006) *Diabetes* **55**, 2153–2156
62. Steiber, A., Kerner, J., and Hoppel, C. L. (2004) *Mol. Aspects Med.* **25**, 455–473
63. Savitha, S., Naveen, B., and Panneerselvam, C. (2007) *Eur. J. Pharmacol.* **574**, 61–65
64. Savitha, S., and Panneerselvam, C. (2007) *Mech. Ageing Dev.* **128**, 206–212
65. Power, R. A., Hulver, M. W., Zhang, J. Y., Dubois, J., Marchand, R. M., Ilkayeva, O., Muoio, D. M., and Mynatt, R. L. (2007) *Diabetologia* **50**, 824–832
66. Noland, R. C., Koves, T. R., Seiler, S. E., Lum, H., Lust, R. M., Ilkayeva, O., Stevens, R. D., Hegardt, F. G., and Muoio, D. M. (2009) *J. Biol. Chem.* **284**, 22840–22852
67. Mingrone, G. (2004) *Ann. N.Y. Acad. Sci.* **1033**, 99–107
68. Ramsay, R. R. (1999) *Am. J. Med. Sci.* **318**, 28–35
69. Schönfeld, P., Dymkowska, D., and Wojtczak, L. (2009) *Free Radic. Biol. Med.* **47**, 503–509
70. Farrell, S. O., Fiol, C. J., Reddy, J. K., and Bieber, L. L. (1984) *J. Biol. Chem.* **259**, 13089–13095
71. Giorgio, M., Migliaccio, E., Orsini, F., Paolucci, D., Moroni, M., Contursi, C., Pelliccia, G., Luzi, L., Minucci, S., Marcaccio, M., Pinton, P., Rizzuto, R., Bernardi, P., Paolucci, F., and Pellicci, P. G. (2005) *Cell* **122**, 221–233
72. Brand, M. D., and Esteves, T. C. (2005) *Cell Metab.* **2**, 85–93
73. Brand, M. D., Pakay, J. L., Ocloo, A., Kokoszka, J., Wallace, D. C., Brookes, P. S., and Cornwall, E. J. (2005) *Biochem. J.* **392**, 353–362